

# Interpreting Psychophysiological States Using Unobtrusive Wearable Sensors in Virtual Reality

Alberto Betella, Daniel Pacheco, Riccardo Zucca, Xerxes D. Arsiwalla, Pedro Omedas  
SPECS, NRAS, Universitat Pompeu Fabra  
Barcelona, Spain  
Email: alberto.betella@upf.edu

Antonio Lanatà, Daniele Mazzei, Alessandro Tognetti, Alberto Greco, Nicola Carbonaro  
Research Centre “E. Piaggio”, University of Pisa  
Pisa, Italy

Johannes Wagner, Florian Lingenfeller  
Human Centered Multimedia, University of Augsburg  
Augsburg, Germany

Elisabeth André  
Human Centered Multimedia, University of Augsburg  
Augsburg, Germany

Danilo De Rossi  
Research Centre “E. Piaggio”, University of Pisa  
Information Engineering Department, University of Pisa  
Pisa, Italy

Paul F.M.J. Verschure  
SPECS, NRAS, Universitat Pompeu Fabra  
ICREA, Institució Catalana de Recerca i Estudis Avançats  
Barcelona, Spain

**Abstract**—One of the main challenges in the study of human behavior is to quantitatively assess the participants’ affective states by measuring their psychophysiological signals in ecologically valid conditions. The quality of the acquired data, in fact, is often poor due to artifacts generated by natural interactions such as full body movements and gestures. We created a technology to address this problem. We enhanced the eXperience Induction Machine (XIM), an immersive space we built to conduct experiments on human behavior, with unobtrusive wearable sensors that measure electrocardiogram, breathing rate and electrodermal response. We conducted an empirical validation where participants wearing these sensors were free to move in the XIM space while exposed to a series of visual stimuli taken from the International Affective Picture System (IAPS). Our main result consists in the quantitative estimation of the arousal range of the affective stimuli through the analysis of participants’ psychophysiological states. Taken together, our findings show that the XIM constitutes a novel tool to study human behavior in life-like conditions.

**Keywords**—Affect analysis, affective states, ecological validity, EDR, HRV, wearable sensors, XIM

## I. INTRODUCTION

In the last two decades, the advances in virtual reality techniques led to their application to a wide range of scientific fields. In particular, virtual reality has been generating

important contributions to scientific research related to the understanding of human behavior [1]. Virtual reality systems, in fact, allow to setup ecologically valid environments where user can act and behave in life-like conditions. At the same time, researchers can have a systematic control of the stimuli presented.

The empirical validation of users’ subjective experience in such environments is commonly conducted through the administration of self-assessment questionnaires. Besides this, the users’ behavioral patterns (e.g., spatial location, gaze, etc.) can be recorded and analyzed, thus offering useful insights on users’ explicit and implicit behavior.

In recent years, due to the improvements in hardware portability, an important addition to the study of human behavior is the measure of psychophysiological signals such as electrodermal response (EDR) and electrocardiogram (ECG). Past literature has shown that these measures are directly related to the Autonomic Nervous System (ANS) and provide means to quantitatively assess a number of human affective states [2], [3], [4].

However, one of the common issues when recording these measures in ecologically valid conditions, is the quality of the signal. As a matter of fact, full body movement and

embodied interaction (e.g., natural gestures) often result in a series of artifacts in the signal that don't allow the extraction of features that assess the users' psychophysiological state. For this reason, there is still a tendency to measure these signals only in conventional lab conditions where the user is sitting or has a limited range of movements and interaction.

To address this problem, we enhanced the eXperience Induction Machine (XIM), an immersive space we constructed to conduct experiments on human behavior, with unobtrusive wearable sensors capable of measuring users' psychophysiological signals [5]. Through this latest addition, we obtained a general-purpose infrastructure to support a broad range of behavioral studies that include human affective states.

We validated our new infrastructure by conducting an experiment where participants were free to move or perform gestures in XIM and, at the same time, were exposed to a series of visual stimuli taken from the International Affective Picture System (IAPS) [6], while recording their ECG and EDR in real-time.

Our results show that we are able to distinguish the arousal range of the stimuli presented to the participants by measuring their psychophysiological signals.

## II. MATERIALS AND METHODS

### A. The eXperience Induction Machine

The XIM (Figure 2) is an immersive space constructed to conduct empirical studies on human behavior in ecologically valid situations that involve full body interaction [7].

The XIM covers an area of about 25 square meters and is equipped with a number of effectors that include 8 projectors, 4 projection screens, a luminous interactive floor and a sonification system.

Along with the effectors, the XIM features a pool of sensors to measure users' explicit and implicit behavior, including a marker-free multi-modal tracking system, floor-based pressure sensors and microphones. Next to these, we added wireless and wearable devices capable of measuring body posture, arm orientation, hand position and fingers movements in real-time, as well as the following psychophysiological signals: ECG, EDR and breathing rate (BR).

In the design of the system, these implicit signals were specifically selected because of their reliability in terms of inference of affective states and because the hardware requirements allowed to mount the sensors on tiny wearable devices.

To provide an ecological form of interaction, the wearable devices were integrated into two main interfaces: a) a sensing glove for the simultaneous acquisition of hand gestures and EDR and b) a sensing shirt for the acquisition of ECG and respiration.

1) *The sensing shirt and glove:* On the one hand, the sensing shirt (Smartex srl, Italy) is used in the XIM to acquire ECG, BR and triaxial accelerometric data [8]. This device has been adopted in previous studies on long-term monitoring of chronic patients, focusing on the early prevention of cardiovascular diseases [9]. The sensing shirt features a front pocket that contains a tiny electronic battery-powered unit that streams the acquired data through a bluetooth connection.

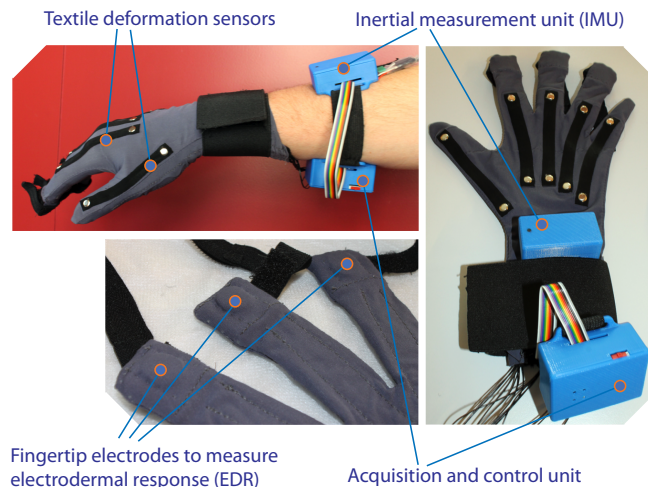


Figure 1. The sensing glove and its main components. See text for further explanation.

On the other hand, the multi-parameter sensing glove (Figure 1) was specifically designed for the XIM space. It measures both explicit and implicit signals (forearm orientation, fingers position and EDR) on a single hand.

In previous work, we demonstrated that textile electrodes are comparable in terms of bio-electric properties to standard Ag/AgCl electrodes [10]. For this reason, in our sensing glove we integrated textile electrodes placed at the fingertips to measure EDR.

In addition, the use of a textile system presents a series of advantages in terms of portability and usability for long-term monitoring, and provides minimal constraints in terms of natural movements and gestures.

Finger motion tracking is obtained through five textile deformation sensors that have been specifically designed and located on the metacarpo-phalangeal hand joints (Figure 1). These sensors, previously used for respiration monitoring in [11], are made of knitted piezoresistive fabric (KPF) material (Smartex srl, Italy). Finger movements produce local deformations in the fabric thus modifying the electrical resistance of the sensors. This resistance is highly correlated with the single finger degree of flexion. The sensor signal is characterized by a slow baseline drift due to the intrinsic characteristics of textile substrate, for this reason a custom-built algorithm for hand gesture recognition was developed [12].

Both EDR and deformation signals are acquired and elaborated in real-time by using a dedicated wearable and wireless electronic unit. Moreover, forearm orientation is measured by an Inertial Measurement Unit (HMC6343, Honeywell, MN, USA) embedded in the glove's electronics and placed on the dorsal area of the forearm, close to the wrist.

2) *The sensing platform:* The data coming from the wearable devices is sent to the XIM sensing platform which is responsible for capturing and processing in real-time raw sensor data [5]. This platform is implemented using the Social Signal Interpretation (SSI) framework [13].

The data stream of each sensor is transmitted through a

dedicated channel and preprocessed (e.g., forearm orientation, fingers position and EDR from the sensing glove are assigned to separate channels).

The sensing platform synchronizes the incoming streams by establishing a stable connection with all the sensors and by eventually starting to buffer the data streams. Each buffer is compared upon regular time intervals according to an internal timestamp and synchronized if necessary. After the synchronization, each one of the signals is processed individually to separate meaningful information from artifacts.

### B. Empirical Validation

1) *Selection of the stimuli*: 12 visual stimuli were chosen from the pictures of the IAPS collection [6], each of which was representing a different rating value of arousal, thus covering the entire scale of arousal from a minimum rating of 1.72 to a maximum of 7.34, as shown in Table I.

2) *Sample and Protocol*: A total of 7 Subjects (4 females, mean age 29.7,  $SD \pm 3.9$ ) participated in the empirical validation.

Prior to the exposure, the participants were helped to wear the sensing shirt and the glove to measure ECG and EDR respectively. A short phase of connection testing followed.

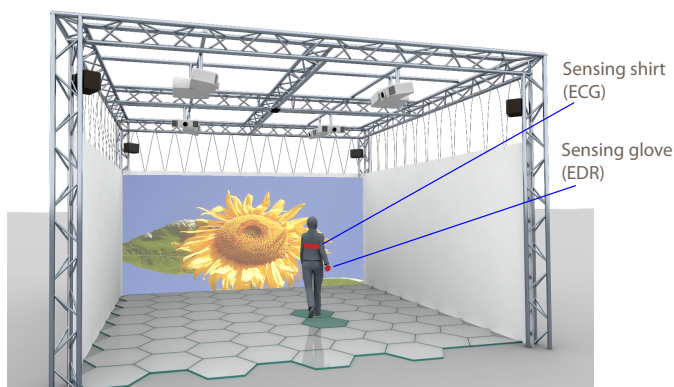


Figure 2. Schematic illustration showing the experimental setting in the eXperience Induction Machine (XIM).

The participants were then instructed to enter the XIM and place themselves at the designated starting point in the center of the room.

A 5-minutes baseline recording phase followed where the participants were asked to maintain a natural standing position and relax as much as possible.

After the baseline recording, the first affective stimulus was displayed on the main screen of the XIM. The order of presentation of the stimuli was randomized for each experimental session.

Each one of the 12 stimuli was displayed for at least 20 seconds, after which a “beep” sound followed to notify the user about the possibility to switch to the following stimulus. To do so, the user was instructed to close all the fingers of the hand wearing the glove, hence generating a “grabbing” event. This event was sent to the sensing platform to provide an accurate

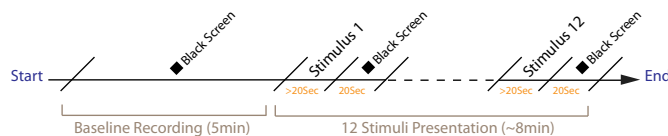


Figure 3. Schematic timeline of a single experimental session.

time marker for each stimulus. A 20-seconds black screen was presented in-between each stimulus (Figure 3).

During the entire experimental session, participants were asked to maintain a standing posture and were free to move when exposed to the visual stimuli (pictures from the IAPS collection) displayed on the main XIM screen (Figure 2).

### C. Acquired Signals

1) *Electrocardiogram*: The ECG signal was used to extract the Heart Rate Variability (HRV) [14], which indicates the time variation between two consecutive R-peaks. Previous research has shown that HRV is directly related to sympatho-vagal balance [2]. To extract HRV, the ECG was pre-filtered using a Moving Average Filter (MAF) to extract and subtract the baseline.

The Heart Rate (HR) is  $HR = \frac{60}{t_{R-R}}$ , where  $t_{R-R}$  is the time interval between two successive R-peaks: consequently, we treated the ECG signal by detecting the QRS complexes through the automatic QRS detection algorithm proposed by Pan-Tompkins [15] and by extracting R-peaks. The obtained HR resulted in a time series sequence of non-uniform RR intervals, hence it was re-sampled in accordance to the recommendations of Berger et al. [16].

2) *Electrodermal Response*: EDR is obtained as the ratio between an imposed continuous voltage of 0.5 V applied to two fingers and flowing current.

EDR is related to variations in the electrical conductance of the skin, due to the changes in the sweat gland activity [17] after a sympathetic stimulation. For this reason hereinafter we refer to EDR as Skin Conductance (SC).

Since sweat gland activity is controlled by the Sympathetic Nerve Activity (SNA) [3], [4], SC constitutes a good measure to monitor changes in the Autonomic Nervous System (ANS). This has been validated in previous studies showing that electrodermal changes are associated to the arousal of the stimuli [18], [19].

The SC signal is characterized by a tonic and a phasic component: the Skin Conductance Level (SCL) and the Skin Conductance Response (SCR) respectively.

On the one hand, SCL is the slowly varying baseline level of skin conductance, related to an overall state of the body. On the other hand, SCR arises within a predefined response window of 1 – 5 seconds after a given stimulus and is directly related to it [20].

Consecutive SCRs can result in an overlap when the inter-stimulus time interval is shorter than SCR recovery time. To address this issue, in this study we adopted a deconvolution model that allows the direct estimation of the SudoMotor

TABLE I. SELECTION OF THE 12 STIMULI FROM THE INTERNATIONAL AFFECTIVE PICTURE SYSTEM (IAPS) DATABASE [6].

ID	IAPS Catalog ID	Description	Arousal mean(SD)	Subset $\alpha$	Subset $\beta$	Subset $\gamma$
1	7175	Lamp	1.72(±1.26)	$A_1$	$A_1$	$A_1$
2	7020	Fan	2.17(±1.71)	$A_1$	$A_1$	$A_1$
3	5030	Flower	2.74(±2.13)	$A_1$	$A_1$	$A_1$
4	7547	Bridge	3.18(±2.01)	$A_1$	-	$A_1$
5	7512	Chess	3.72(±2.07)	$A_1$	-	$A_2$
6	9280	Smoke	4.26(±2.44)	-	-	$A_2$
7	9171	Fisherman	4.72(±2.17)	-	-	$A_2$
8	9582	Dental Exam	5.29(±2.21)	$A_2$	-	$A_2$
9	9611	Plane Crash	5.75(±2.44)	$A_2$	-	$A_3$
10	9622	Jet	6.26(±1.98)	$A_2$	$A_2$	$A_3$
11	9412	Dead Man	6.72(±2.07)	$A_2$	$A_2$	$A_3$
12	3000	Mutilation	7.34(±2.27)	$A_2$	$A_2$	$A_3$

Nerve Activity (SMNA) which is the controller of the eccrine sweat glands activity [21]. The SMNA shows an inter-stimulus time interval shorter than the SCR signal thus avoids the overlapping problem. Specifically, the SCR is the result of a convolution model between SMNA and the following biexponential Impulse Response Function (IRF), which is called Bateman function [22]:

$$IRF(t) = (e^{-\frac{t}{\tau_1}} - e^{-\frac{t}{\tau_2}}) \cdot u(t) \tag{1}$$

where  $u(t)$  is the step function. This function is characterized by a rapid increase and a slower recovery. More specifically,  $\tau_1$  is a time constant that describes the rapid slope, taking information on time course of the evacuation of sweat from the compartment model, while  $\tau_2$  is the related slow recovery slope.

D. Physiological features

1) *Heart Rate Variability*: HRV is related to the time intervals between heartbeats [14].

A number of features were extracted in both the time and the frequency domains. In the time domain, we extracted statistical parameters and morphological indices. We fixed a time window (NN) and extracted the following features: a) simple MNN and SDNN, which correspond to the mean value and to the standard deviation of the NN intervals, respectively, b) the root mean square of successive differences of intervals (RMSSD) and c) the number of successive differences of intervals which differ by more than 50 ms (pNN50 % expressed as a percentage of the total number of heartbeats analyzed).

In the HRV frequency domain analysis, three main spectral components were distinguished in a spectrum calculated from short-term recordings: Very Low Frequency (VLF), Low Frequency (LF), and High Frequency (HF) components. Short terms recordings are intended as the time duration of HRV signal segments. In this work HRV segments were in agreement with picture presentation time. Current HRV research in the frequency domain analysis suggests that even though the frequency band division represents a unique, non-invasive tool to achieve an assessment of autonomic function, the use of HF and LF components does not allow to precisely assess the state of sympathetic activation. Therefore, along with the estimation of the Power Spectral Density in the VLF, LF, and HF band, we also calculated the LF/HF PSD Ratio which provides information about the Sympatho-Vagal balance [23] (Table II).

2) *Skin Conductance*: SC decomposition to its components was performed using Ledalab software package in MATLAB [24]. The signal was filtered by means of a low pass zero-phase forward and reverse digital filter [25] with a cutoff frequency of 2 Hz.

The phasic features were calculated within a time window (response window) of 5 seconds length after stimulus onset. We extracted the number of SCRs within the response window (nSCR), the latency of the first SCR (Lat), the Amplitude-Sum of SCRs (reconvolved from phasic driver-peaks) (AmpSum), the average phasic driver activity (Mean.SCR) (time integral over response window by size of response window), the variance of the phasic driver signal (Var.SCR), the Phasic driver area under curve (AUC.SCR) and the max phasic driver amplitude (Max.SCR).

From the tonic driver signal we extracted the following features: average level of (decomposed) tonic component (Mean.Tonic), variance of the tonic driver signal (Var.Tonic) and number of the non-specific response (i.e., the spontaneous skin conductance response unrelated to a specific stimulus) (NSR) (Table II).

TABLE II. FEATURES EXTRACTED FROM HRV AND SC.

Feature set	Signals
MNN, SDNN, RMSSD, pNN50, VLF, LF, HF, LF/HF	HRV
Lat, nSCR, Mean.SCR, Var.SCR, Max.SCR, AmpSum, AUC.SCR, Mean.Tonic, Var.Tonic, NSR	SC

E. Data Analysis

A number of fixed windows were used to segment the signals (EDR, HRV) in accordance to the experimental protocol (Section II-B2). On the one hand, to compute each feature of the phasic component, the EDR signal was segmented using a 5 seconds window starting after the presentation of each black screen that anticipates the IAPS image. On the other hand, longer windows of 20 seconds length (i.e., the entire duration of each one of the 12 stimuli) were used to compute the HRV parameters.

The extracted features (Table II) were normalized in accordance to the baseline recording. Subsequently, the dataset was divided into 3 different subsets as follows:

- $\alpha$ :  $A_1$  refers to arousal intervals 1-3,  $A_2$  refers to arousal intervals 5-7. Each class comprises 5 stimuli.

- $\beta$ :  $A_1$  refers to arousal intervals 1-2,  $A_2$  refers to arousal intervals 6-7. Each class comprises 3 stimuli.
- $\gamma$ :  $A_1$  refers to arousal intervals 1-3,  $A_2$  refers to arousal intervals 3-5,  $A_3$  refers to arousal intervals 5-7. Each class comprises 4 stimuli.

As a result, the subsets  $\alpha$  and  $\beta$  represent a 2-class problem, while subset  $\gamma$  represents a 3-class problem (Table I).

A statistical inference analysis was conducted by means of non-parametric tests due to the non-gaussianity of the sample set to verify the null-hypothesis of having no statistical difference between the classes for both the 2-class (datasets  $\alpha$  and  $\beta$ ) and the 3-class (dataset  $\gamma$ ) problems.

The  $\alpha$  and the  $\beta$  datasets were submitted to a Mann-Whitney test. Instead, the  $\gamma$  dataset was submitted to a Kruskal-Wallis (KW) test, and a subsequent pairwise comparison among  $A_1$ ,  $A_2$  and  $A_3$ , was performed by means of Mann-Whitney tests with a Bonferroni correction.

#### F. Pattern Recognition

The pattern recognition process aimed to investigate whether the arousal sessions could be distinguished in both the 2-class and the 3-class recognition problems.

Taking into account the entire dataset of features, the dimension of the features space was reduced through the application of the Principal Component Analysis (PCA) where we consider the number of PCs that explain 90% of the total variance.

In this work, the classification stage was performed in order to classify each sample of the dataset according to the set of classes reported in Section II-E.

We tested the following classifiers: Linear Discriminant Classifier (LDC), Quadratic Discriminant Classifier (QDC), Mixture Of Gaussian (MOG), k-Nearest Neighbor (k-NN), Kohonen Self Organizing Map (KSOM), Multilayer Perceptron (MLP) and Nearest Mean Classifier (NMC) [26], [27], [28].

Among the aforementioned classifiers, the LCD [29] showed the highest recognition accuracy and consistency in arousal discrimination. For this reason, and for the sake of brevity, here we limit the report and discussion of our results to the LCD. The performance of the classification process was examined using the confusion matrix, which represents the capacity of the algorithm to recognize each sample as belonging to one of the predefined classes. In details, a more diagonal confusion matrix corresponds to a higher degree of classification.

Here, we used a training set of 80% of the whole features dataset while the remaining 20% was used as testing set. The validity of the classification model was evaluated using computational techniques and, in particular, the cross-validation method. More specifically, we performed 40-fold cross-validation steps in order to obtain unbiased results. The final results were expressed as the mean and the standard deviation of the 40 computed confusion matrices.

TABLE III. CONFUSION MATRIX OF THE LDC CLASSIFIER FOR THE 2-CLASS PROBLEM FOR  $\alpha$  AND  $\beta$  DATASETS. THE RESULTS WERE OBTAINED AFTER 40 CROSS-FOLD VALIDATIONS.

LDC	Dataset $\alpha$		Dataset $\beta$	
	$A_1$	$A_2$	$A_1$	$A_2$
$A_1$	<b>87.27±6.19</b>	7.72±15.12	<b>95.36±6.77</b>	0.00±0.00
$A_2$	12.72±6.19	<b>92.27±15.12</b>	4.64±6.77	<b>100.0±0.00</b>

TABLE IV. CONFUSION MATRIX OF THE LDC CLASSIFIER FOR THE 3-CLASS PROBLEM FOR  $\gamma$  DATASET. THE RESULTS WERE OBTAINED AFTER 40 CROSS-FOLD VALIDATIONS.

LDC	$A_1$	$A_2$	$A_3$
$A_1$	<b>88.89±10.19</b>	2.78±6.11	5.56±10.44
$A_2$	7.72±6.11	<b>85.56±12.01</b>	21.11±13.74
$A_3$	3.89±5.43	11.67±11.09	<b>73.33±11.29</b>

### III. RESULTS

An intra-subject analysis was performed for all the subjects and all the extracted features.

No statistically significant features were found in the  $\alpha$  dataset, while for the  $\beta$  dataset we found a significant difference in the LF feature ( $p < .05$ ) between the two classes  $A_1$  and  $A_2$ . The Kruskal-Wallis (KW) test (Section II-E) indicated a statistical difference among the three classes  $A_1$ ,  $A_2$  and  $A_3$  of the  $\gamma$  dataset. The pairwise comparison showed that both the features RMSSD and HF were significantly different in the three classes ( $p < .01$ ).

As a result of the pattern recognition phase (Section II-F), the LDC classifier accounted for a high accuracy in the recognition of both the 2-class and the 3-class problems (Tables III and IV respectively).

### IV. CONCLUSION

To address the question of how known emotional responses that have been established under standard laboratory conditions generalize to ecologically valid environments, we enhanced the eXperience Induction Machine (XIM) with unobtrusive wearable sensors: the sensing shirt and the sensing glove. These devices allow to measure human behavioral patterns (e.g., body posture, finger movements, etc.) as well as a number of psychophysiological signals (ECG, BR, EDR).

To validate our augmented infrastructure, we conducted an experiment in the XIM where participants were exposed to a series of visual stimuli taken from the IAPS collection, while wearing the sensing shirt and glove without any physical constraint (i.e., they were able to move freely in the space and to perform gestures).

Our results show that a number of HRV-extracted features (LF, RMSSD, HF) were coherent with the arousal ratings of the stimuli. Although the statistical significance obtained was limited to a small set of features, accuracy was high. A multivariate analysis with a LDC considering the entire dataset accounted for an accuracy between 73.3% and 88.9% in the 3-class problem, and exceeding 87% in the 2-class problem. An implication of our findings is the possibility to recognize users' level of arousal in the XIM with a high accuracy.

The addition of tailored-made solutions (e.g., the sensing glove) to the XIM infrastructure constitutes a novel approach

when compared to similar devices to measure psychophysiological states, such as the Q Curve by Affectiva Inc. [30]. Our system as a whole offers a higher number of parameters that can be measured, as well as a higher level of integration and future extensibility.

Taken together, our results show that XIM constitutes an ideal tool to study human behavior in ecologically valid conditions by acquiring both explicit and implicit measures.

Future improvements will consist in empirical validations of our system in more complex life-like conditions (e.g., fast walking, elaborate gestures and body postures, etc.).

## V. ACKNOWLEDGEMENT

The research leading to these results has received funding from the European Community's Seventh Framework Programme (FP7-ICT-2009-5) under grant agreement n. 258749 [CEEDS]. The Generalitat de Catalunya (CUR, DIUE) and the European Social Fund are supporting this research.

## REFERENCES

- [1] C. J. Bohil, B. Alicea, and F. a. Biocca, "Virtual reality in neuroscience research and therapy," *Nature Reviews Neuroscience*, vol. 12, no. December, Nov. 2011.
- [2] P. Stein, M. Bosner, R. Kleiger, and B. Conger, "Heart rate variability: a measure of cardiac autonomic tone," *American Heart Journal*, vol. 127, no. 5, 1994, pp. 1376–1381.
- [3] D. Fowles, M. Christie, R. Edelberg, W. Grings, D. Lykken, and P. Venables, "Publication recommendations for electrodermal measurements," *Psychophysiology*, vol. 18, no. 3, 1981, pp. 232–239.
- [4] W. Boucsein, *Electrodermal activity*. Springer Verlag, 2011.
- [5] J. Wagner, F. Lingenfeller, E. André, D. Mazzei, A. Tognetti, A. Lanatà, D. De Rossi, A. Betella, R. Zucca, P. Omedas, and P. F. M. J. Verschure, "A sensing architecture for empathetic data systems," in *Proceedings of the 4th Augmented Human International Conference*, ser. AH '13. New York, NY, USA: ACM, 2013, pp. 96–99.
- [6] P. J. Lang, M. M. Bradley, and B. N. Cuthbert, "International affective picture system (IAPS): Affective ratings of pictures and instruction manual," *The Center for Research in Psychophysiology*, University of Florida, Gainesville, FL, Tech. Rep. A-8, 2008.
- [7] U. Bernardet, A. Våljamäe, M. Inderbitzin, S. Wierenga, A. Mura, and P. F. M. J. Verschure, "Quantifying human subjective experience and social interaction using the eXperience Induction Machine," *Brain research bulletin*, vol. 85, Nov. 2010, pp. 305–312.
- [8] R. Paradiso, G. Loriga, and N. Taccini, "A wearable health care system based on knitted integrated sensors," *Information Technology in Biomedicine*, *IEEE Transactions on*, vol. 9, no. 3, 2005, pp. 337–344.
- [9] E. Scilingo, A. Gemignani, R. Paradiso, N. Taccini, B. Ghelarducci, and D. De Rossi, "Performance evaluation of sensing fabrics for monitoring physiological and biomechanical variables," *Information Technology in Biomedicine*, *IEEE Transactions on*, vol. 9, no. 3, 2005, pp. 345–352.
- [10] A. Lanatà, G. Valenza, and E. Scilingo, "A novel EDA glove based on textile-integrated electrodes for affective computing," *Medical & Biological Engineering & Computing*, vol. 50, no. 11, 2012, pp. 1163–1172.
- [11] R. Paradiso and L. Caldani, "Electronic textile platforms for monitoring in a natural environment," *Research Journal of Textile and Apparel*, vol. 14, no. 4, 2010.
- [12] N. Carbonaro, A. Greco, G. Anania, G. Dalle Mura, A. Tognetti, E. P. Scilingo, D. De Rossi, and A. Lanatà, "Unobtrusive Physiological and Gesture Wearable Acquisition System: A Preliminary Study on Behavioral and Emotional Correlations," in *GLOBAL HEALTH 2012, The First International Conference on Global Health Challenges*, 2012, pp. 88–92.
- [13] J. Wagner, F. Lingenfeller, T. Baur, I. Damian, F. Kistler, and E. André, "The Social Signal Interpretation (SSI) Framework: Multimodal Signal Processing and Recognition in Real-time," in *Proceedings of the 21st ACM International Conference on Multimedia*, ser. MM '13. New York, NY, USA: ACM, 2013, pp. 831–834. [Online]. Available: <http://doi.acm.org/10.1145/2502081.2502223>
- [14] U. Rajendra Acharya, K. Paul Joseph, N. Kannathal, C. Lim, and J. Suri, "Heart rate variability: a review," *Medical and Biological Engineering and Computing*, vol. 44, no. 12, 2006, pp. 1031–1051.
- [15] J. Pan and W. Tompkins, "A real-time QRS detection algorithm," *IEEE Transactions on Biomedical Engineering*, 1985, pp. 230–236.
- [16] R. Berger, S. Akselrod, D. Gordon, and R. Cohen, "An efficient algorithm for spectral analysis of heart rate variability," *Biomedical Engineering*, *IEEE Transactions on*, no. 9, 2007, pp. 900–904.
- [17] W. Winton, L. Putnam, and R. Krauss, "Facial and autonomic manifestations of the dimensional structure of emotion," *Journal of Experimental Social Psychology*, vol. 20, no. 3, 1984, pp. 195–216.
- [18] P. Lang, M. Greenwald, M. Bradley, and A. Hamm, "Looking at pictures: Affective, facial, visceral, and behavioral reactions," *Psychophysiology*, vol. 30, no. 3, 1993, pp. 261–273.
- [19] P. Lang, "The emotion probe," *American Psychologist*, vol. 50, no. 5, 1995, pp. 372–385.
- [20] D. Levinson and R. Edelberg, "Scoring criteria for response latency and habituation in electrodermal research: a critique," *Psychophysiology*, vol. 22, no. 4, 1985, pp. 417–426.
- [21] M. Benedek and C. Kaernbach, "A continuous measure of phasic electrodermal activity," *Journal of neuroscience methods*, vol. 190, no. 1, 2010, pp. 80–91.
- [22] E. Garrett, "The bateman function revisited: a critical reevaluation of the quantitative expressions to characterize concentrations in the one compartment body model as a function of time with first-order invasion and first-order elimination," *Journal of Pharmacokinetics and Pharmacodynamics*, vol. 22, no. 2, 1994, pp. 103–128.
- [23] A. Camm, M. Malik, J. Bigger, G. Breithardt, S. Cerutti, R. Cohen, P. Coumel, E. Fallen, H. Kennedy, R. Kleiger et al., "Heart rate variability: standards of measurement, physiological interpretation, and clinical use," *Circulation*, vol. 93, no. 5, 1996, pp. 1043–1065.
- [24] M. Benedek and C. Kaernbach, "Decomposition of skin conductance data by means of nonnegative deconvolution," *Psychophysiology*, vol. 47, no. 4, 2010, pp. 647–658.
- [25] S. Mitra, "Digital signal processing. a computer-based approach. 2001."
- [26] F. Heijden, R. Duin, D. Ridder, and D. Tax, *Classification, Parameter Estimation and State Estimation*. John Wiley, 2004.
- [27] R. Duda, P. Hart, and D. Stork, *Pattern classification*. 2nd edition, John Wiley and Sons, 2001.
- [28] J. Friedman, T. Hastie, and R. Tibshirani, "Additive logistic regression: A statistical view of boosting," *The Annals of Statistics*, vol. 38, no. 2, 2000, p. 337 374.
- [29] W. Hrdle and L. Simar, *Applied multivariate statistical analysis*. Springer, 2007.
- [30] Affectiva Inc., "Liberate yourself from the lab : Q Sensor measures EDA in the wild (White Paper)," 2012.